Water Air Soil Pollut (2025) 236:578
https://doi.org/10.1007/s11270-025-08189-3

Antimicrobial and Photocatalytic Potential of a Composite of ZnO-ZnS and Activated Carbon Obtained From Banana Peel

Marta Mediavilla · Luis Fernando Valencia · Claudia L Quiroz-Vela · Henry Zúñiga-Benítez · Aída Luz Villa · Gustavo A. Peñuela

Received: 23 November 2024 / Accepted: 21 May 2025 / Published online: 12 June 2025

Abstract Banana peel was mixed with zinc sulfate and pyrolyzed at 500 °C under nitrogen to synthesize a composite with potential antibacterial activity against both Gram-positive *Escherichia coli* and Gram-negative *Staphylococcus aureus*. The material was characterized by TGA, nitrogen adsorption-desorption isotherm, SEM-EDX, DRX, DRS UV-Vis, and DLS. XRD analysis showed the presence of ZnO and ZnS in the composite, and TGA analysis revealed the presence of lignocellulosic material in the solid due to decomposition peaks characteristic of hemicellulose, cellulose, and lignin. Nitrogen adsorption and desorption isotherm analysis revealed a surface area of 165.0 m^2/g, an average pore diameter of 16.0 nm, and a total pore volume of 0.16 cm^3/g. C, O, Zn, and Si were determined as the most significant elements present in the material. DLS showed a distribution with a single type of particle. UV-Vis analysis revealed an Eg value of 2.0 eV for the composite, indicating potential antibacterial properties and suitability for biomedical applications. The use of the material in removing sildenafil, an emerging contaminant present in various environmental matrices, was evaluated, considering the effects of parameters such as the solution pH, the catalyst dosage, and the reuse of the composite over five cycles. The composite obtained from agro-industrial waste is a promising material to remove organic contaminants from water.

Highlights
- A composite derived from banana peel and zinc sulphate was obtained
- The synthesized composite shows micro and mesoporosity
- The band gap of the composite was 2.0 eV
- The composite exhibits potential antimicrobial activity
- Sildenafil was removed using the composite and simulated sunlight

Keywords Antibacterial activity · Banana waste · Composites · Photocatalysis · Sildenafil · Wastewater treatment

M. Mediavilla
Engineering Faculty, Universidad Central de Venezuela, Caracas, Venezuela

M. Mediavilla (✉) · L. F. Valencia · A. L. Villa (✉)
Chemical Engineering Department, Environmental Catalysis Research Group, Universidad de Antioquia, Medellín, Antioquia, Colombia
e-mail: qmarta338@gmail.com

A. L. Villa
e-mail: aida.villa@udea.edu.co

C. L. Quiroz-Vela · H. Zúñiga-Benítez · G. A. Peñuela
Grupo GDCON, Facultad de Ingeniería, Sede de Investigación Universitaria (SIU), Universidad de Antioquia UdeA, Calle 70 # 52-21, Medellín, Colombia

H. Zúñiga-Benítez
Departamento de Ingeniería Química, Facultad de Ingeniería, Universidad de Antioquia UdeA, Calle 70 # 52-21, Medellín, Colombia

1 Introduction

According to the World Health Organization, the health repercussions of the climate crisis, water pollution, food safety issues, and the increasing number of disease outbreaks are some of the most significant problems facing humanity and the planet today. For example, problems related to antimicrobial resistance cause five million human deaths yearly, and by 2050, economic losses of up to USD 100 billion are expected (World Health Organization (WHO), 2023). Another problem is the presence of pharmaceutical compounds in water, such as sildenafil (SDF), which is used to treat erectile dysfunction and pulmonary arterial hypertension (Zizzamia et al., 2024). It is also an active ingredient used to treat hypoxia, pulmonary hypertension in newborns, and cardiovascular diseases. The massive use of SDF has spread due to the lack of control regarding its sales; in many countries, it is used by young people (20 to 30 years old) deliberately for recreational purposes or to increase their sexual potency (Barna et al., 2023; Zeng et al., 2023; Zizzamia et al., 2024). Because the human body does not completely metabolize SDF and treatment plants are not properly designed, the presence of SDF has been reported in several bodies of water, which represents a potential risk to aquatic ecosystems and to the species that inhabit them (Zizzamia et al., 2024).

Every year, a massive amount of waste is generated, requiring efficient solutions to manage it. Inaction on global waste management negatively affect human health, economies, and the environment; it is projected losses of around USD 600 billion per year by 2050 because inappropriate manage of wastes (United Nations (UN) Environment program, 2024). Banana peels are often discarded as waste, contributing to environmental pollution and greenhouse gas emissions when decomposing in landfills. However, these peels have been utilized as organic fertilizers, biosorbents, pharmacological agents, animal feed, and in energy production (Atilgan et al., 2023; Farias et al., 2023; Korni et al., 2023; Melanie et al., 2024; Mishra et al., 2023). These wastes are rich in organic compounds, such as cellulose, hemicellulose, and lignin, which could be employed to develop eco-friendly and sustainable valuable products (Serna-Jiménez et al., 2023).

Many pathogenic bacteria are widely distributed in nature, aquatic, and animal reservoirs. *Escherichia coli* and *Staphylococcus aureus* have been identified as the main etiological agents responsible for foodborne disease outbreaks. These bacteria are associated with urinary tract infections, cholecystitis or septicemia, toxic shock syndrome, endocarditis, and post-operative wound infections (Singh et al., 2002). Some studies have highlighted the use of lignocellulosic materials as antibacterial agents (Das et al., 2024; Huët et al., 2024; Li et al., 2023; Lobo et al., 2021; Luo et al., 2020). Lobo et al. (2021) published an update of the studies that illustrate the potential of lignocellulosic-based materials as antimicrobial agents, highlighting their application as novel drug-free antibacterial polymers. Gomez et al. (2024) reported a review about the use of metal-organic frameworks (MOFs) and metallic oxide mesoporous as antibacterial agents, and although this MOFs application is still in preliminary phases, these materials offer favorable attributes for being used in biomedicine and human health.

Natural and food waste (nonedible), acting as bio-templates, have been used with zinc salts to synthesize materials made of ZnO that show an increased efficiency for CO_2 valorization (Garay-Rodríguez et al., 2023). Bianchini et al. (2023) reported that Zn-based materials exhibit antiseptic and antimicrobial properties with potential for biomedical applications. ZnO has anti-microbial and anti-biofilm activity on a wide range of bacteria; meanwhile, ZnS has shown high efficacy on bacterial planktonic and biofilm inhibition, suggesting the possibility of being applied in medicine and food industry. Additionally, Chankhanittha et al. (2023) reported that the heterojunction of ZnO/ZnS has a high potential for completely removing organic pollutants from aqueous matrices. Pullapukuri and Kumar (2023) synthesized ZnO nanoparticles utilizing banana peel extract, which exhibited antibacterial activity against the gram-negative (*V. cholerae*, *S. flexneri*, and *Enterobacter aerogenes*), and gram-positive bacteria (*Staphylococcus aureus*, *C. glutamicum,* and *Clostridium perfringens*). T-Thienprasert et al. (2021) highlighted the green synthesis of ZnO nanoparticles using banana peel extract. The material showed a higher growth inhibition of the fungus *Colletotrichum* sp. present in orchid plants and a significant reduction of anthracnose symptoms on inoculated orchid leaves. Also, ZnS nanoparticles derived from banana peel waste exhibit promising optical properties, including strong absorption in the UV region (260–300 nm) and luminescence behavior in the visible region, which suggests potential applications in various optoelectronic devices (Bisauriya et al., 2018). Recently, Alphanoda et al. (2024) synthesized porous hydrochar from banana peel using temperatures ranging from 180 °C to 270 °C; the resulting materials were utilized as a photoelectrochemical system for hydrogen production under visible light. The authors reported a hydrogen production of 1566.05 μmol/g with the hydrochar obtained at 270 °C. The combination of agro-industrial waste with zinc salts for generating new materials has the potential to minimize the negative environmental impacts associated with the contamination and depletion of natural resources (Zeghoud et al., 2022). Its applications, for example, include healthcare, agriculture, and water treatment, providing an opportunity to repurpose and add value to waste and reduce the environmental impact of disposal (Nesterov et al., 2024). Eswaran et al. (2024) synthesized a ZnO/BC nanocomposite from banana peels and $Zn(OAc)_2.2H_2O$, achieving 92% photocatalytic degradation of methylene blue with the synthesized material under sunlight irradiation after 120 minutes. Furthermore, Zn(O, S)/C composite (Abdullah et al., 2022) was synthesized from banana peels, urea, and potassium carbonate mixture, this material showed photocatalytic activity (under simulated solar light irradiation, 5 h) for hydrogen generation of 9232 mmol/g.

This work reports the synthesis of a new composite from banana peel and zinc sulfate prepared from pyrolysis at 500 °C. The solid was characterized by TGA, XRD, nitrogen physisorption, SEM-EDX, DLS, and DRS UV-Vis. The agar-well diffusion test was used to explore the material's antibacterial activity against *E. coli* and *S. Aureus*. In addition, the potential application of the composite in removing the organic contaminant sildenafil from water using photocatalysis was also assessed.

2 Methodology

2.1 Materials

Banana peels were collected from a local supplier (Medellín, Colombia). Merck supplied analytical grade $ZnSO_4.7H_2O$. Ethyl-alcohol was purchased from J. T. Baker, and nitrogen gas UPA (99.999%) was obtained from Messer. *E. coli* and *S. aureus* were obtained from the Universidad de Antioquia microbiological labs.

2.2 Composite Preparation

Composite from banana peels and zinc sulfate was obtained using the one-step method (Villa & Medi-avilla, 2023). The methodology involves drying banana peels at 80 °C for 24 h, followed by pulverization to obtain a fine powder. This powder is then mixed with 20 mL of water and subjected to microwave heating from room temperature to 50 °C at a rate of 10 °C/min, after which it is held at 50 °C for 3 min. The material, once dried, was treated with an aqueous solution of $ZnSO_4.7H_2O$ (1.4 M) using an activating agent/peel weight ratio of 2:1, then it was kept at room temperature for 24 h. The resulting paste was dried in an air oven at 100 °C for 18 h and then pyrolyzed in a nitrogen flow (100 mL/min) at 500 °C. The obtained composite was washed with ethanol and hot water and finally dried.

2.3 Composite Characterization

TGA of materials was carried out by a thermogravimetric analyzer (SDT-Q600, TA Instruments) from 30 °C to 800 °C under N_2 flow, and then the atmosphere was switched to air for 25 min. XRD patterns of samples were recorded using an X-ray diffractometer (Philips, X'Pert) and Cu-Kα radiation ($\lambda = 0.1542$ nm) over a diffraction angle range of 2θ from 10 to 80 °. The surface and textural properties of the obtained activated carbon were determined from the adsorption-desorption isotherms using nitrogen as adsorbate (ASAP 2020 PLUS, Micromeritics); the samples were degassed at low pressure and at 350 °C for 4 h, and adsorption isotherms were obtained by immersing sample tubes in liquid nitrogen (77 K) to achieve constant temperature conditions. SEM (JEOL JSM 6490 LV) was used to evaluate the activated carbon morphology, and the elemental compositions were analyzed by EDX (INCA PentaFETx3 Oxford Instruments). The samples were fixed to a graphite tape, coated with gold, and analyzed in a high vacuum scanning electron microscope operating at 20 kV. A Shimadzu UV-Vis-2600 equipped with an integrating sphere ISR-2600 Plus was used to obtain the UV-Vis diffuse reflectance spectra in the wavelength range of 200–1400 nm; $BaSO_4$ was used as a reference. Finally, the size distribution profile of the composite was determined using a Mastersizer 2000 (Malvern Instrument) and water as dispersing medium under a size range from 0.020 µm to 2000 µm.

2.4 Photocatalytic Experiments

SDF was chosen as a model molecule to evaluate the potential use of the agro-industrial composite in water treatment. All reagents were of analytical grade, and solutions were prepared using ultra-pure water obtained from a Millipore Direct-Q 3 UV Water Purification System (18.2 MΩ•cm). Experiments were carried out using a Suntest CPS+ (Atlas) photosimulator (wavelength between 290 and 800 nm and irradiance of 500 W/m^2). Borosilicate glass flasks containing 50 mL of 1 mg/L SDF aqueous solution were used for light exposition; a specific amount of catalyst was added to obtain its desired concentration under selected pH conditions and a stirring speed of 300 rpm. In most cases, the reaction time was 90 minutes. The effects of the solution pH and the catalyst dose were studied. In addition to the photocatalytic test, some controls, including photolysis and adsorption, were done to clarify the pollutant elimination mechanism. Isopropanol and acetonitrile were used as scavenger agents to identify the role of photo-generated species on SDF degradation.

Samples were withdrawn at different intervals to monitor and follow the pollutant concentration in the treated solutions. Liquid chromatography coupled to tandem mass spectrometry (LC-MS/MS), using an ultra-high efficiency UHPLC equipment (Waters Corporation) and an Agilent 6460 triple quadrupole mass spectrometer (UHPLC-QqQ MS/MS), together with a Kinetex C18 2.6 µm 2.1 x 100 mm Synergi HPLC column (Phenomenex, USA) were part of the analytical equipment. Chromatographic solvents were methanol, water, and ammonium acetate. Furthermore, five water treatment cycles were considered to evaluate the possibility of reusing the composite in the photocatalytic reaction.

2.5 Antibacterial Assessment

The evaluation of antimicrobial activity was performed with composite discs (10 and 25 mg) against *E. Coli* (gram-negative) and *S. Aureus* (gram-positive) bacteria by the disc diffusion test in a Müller-Hinton agar, following the Kirby-Bauer method (Midolo et al., 1995). The microbial suspensions were spread over the Petri plate surface; the negative control was bacterial strains, and the positive was tetracycline (30 µg). The antimicrobial performance was determined by considering the formation of inhibition halos around the composite discs, and the experiments were performed in triplicate.

3 Results and Discussion

3.1 Material Characterization

Figure 1 depicts the thermal stability of the obtained material. TGA/DTG curve shows an initial weight loss at 84 °C, which corresponds to water evaporation; then, it is observed a weight loss between 150 and 800 °C that could be assigned to hemicellulose (212 °C), cellulose (385 °C), and lignin (587 °C) from banana peel, which remained even after thermal treatment with nitrogen at 500 °C. The solid obtained shows a higher thermal stability than the material reported by Anyama et al. (2021) who studied the structural and photocatalytic properties of a zinc (II) coordination polymer based on 1,3,5-benzene tricarboxylic acid and the derived nanocomposites from activated carbon obtained from banana and orange peels. The authors reported that the obtained TGA curve showed weight losses at 221 °C and 328 °C corresponding to the decomposition of hemicellulose and lignocellulose, respectively.

Figure 2a and b present the textural properties of the obtained composite. According to the International Union of Pure and Applied Chemistry classification, the isotherm is a combination of type I and type IV, that is typical of microporous and mesoporous solids with a sharp hysteresis loop that indicates the narrow pore distribution with a calculated pore diameter of 16.0 nm. The specific surface area was 165 m^2/g, and the pore volume was 0.16 cm^3/g. Mesoporous materials have been reported as suitable candidates for applications in inhibiting the growth of pathogenic bacteria. Zhang et al. (2014) reported that mesoporous nanoparticles of ZnO have a high antibacterial activity against *E. coli* and *S. aureus.*

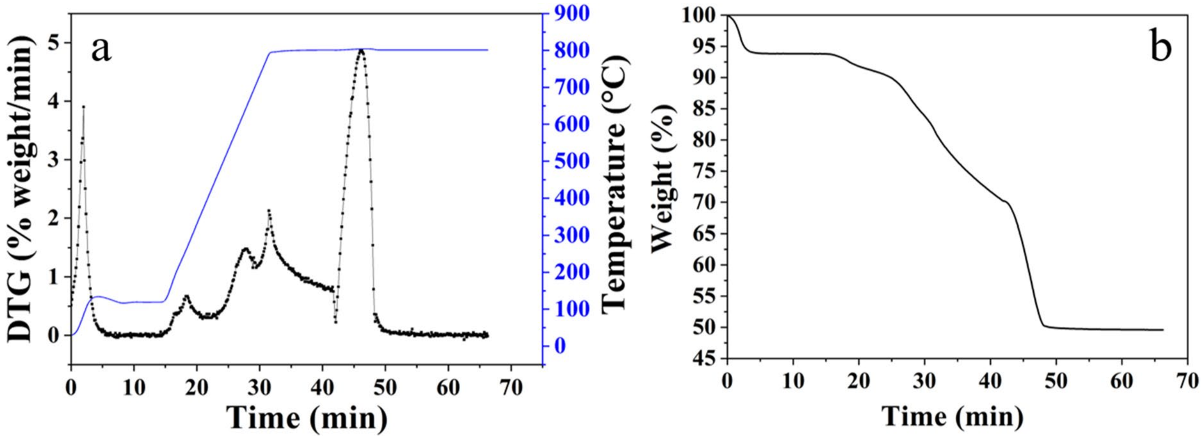

Fig. 1 **a** TGA, **b** DTG curves of the synthesized composite

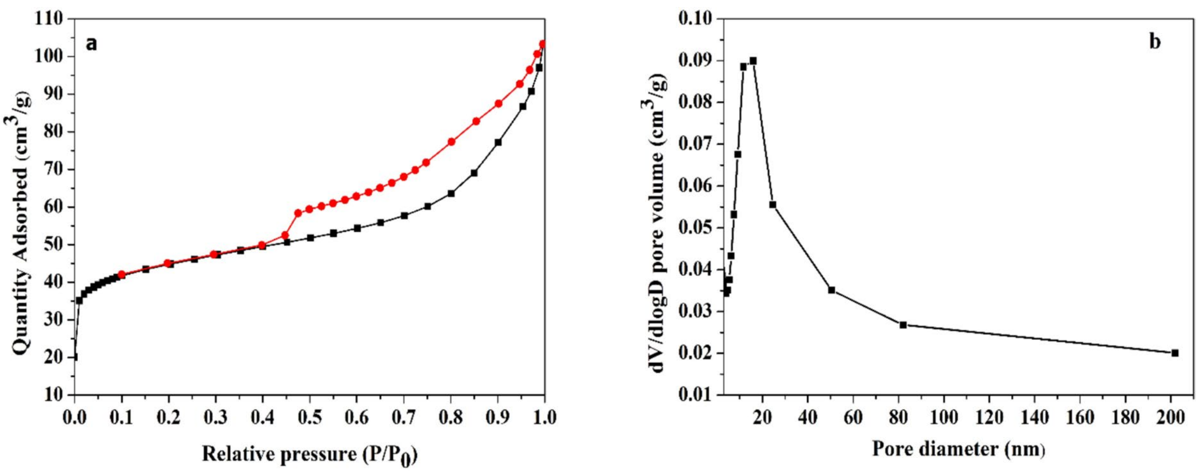

Fig. 2 **a** Adsorption-desorption isotherm, **b** pore size distribution of the synthesized composite

DLS was used to measure the size distribution of the material. Figure 3. shows the distribution by volume of the solid particles, which confirms the absence of aggregates in the composite.

Figure 4 shows the synthesized composite's representative SEM images; they indicate that the surface of the composite is porous and smooth, with deep holes and grooves. The presence of irregularly shaped agglomerates allows us to infer the effective blending of zinc species and the carbonaceous matrix. The chemical composition analysis obtained by EDX showed a high content of C, O, Zn, and Si, followed by S, Ca, and K. All elements show a homogeneous distribution on the surface.

In Fig. 5, that presents the composite's XRD pattern, it is observed that the peaks at 2θ values of 31.7°, 34.4°, 36.2°, 47.4°, 56.5°, 62.7°, 67.8°, 68.9°, and 76.9° are intense, indicating that the samples are crystalline and correspond with ZnO hexagonal nanoparticle indexes according to the PDF database 98006-7848. The minor peaks at 28.9°, 47.4°, and 56.5° could be assigned to ZnS, as reported by Ali et al. (2020). The results confirmed the presence of ZnO-ZnS on the carbon surface, in accordance with the EDX mapping results. The higher zinc concentration (45.43%) compared to the carbon content (16.72%) indicates that the predominant phase in the composite is ZnO. The formation of ZnO-ZnS by thermal decomposition of $ZnSO_4$ was reported

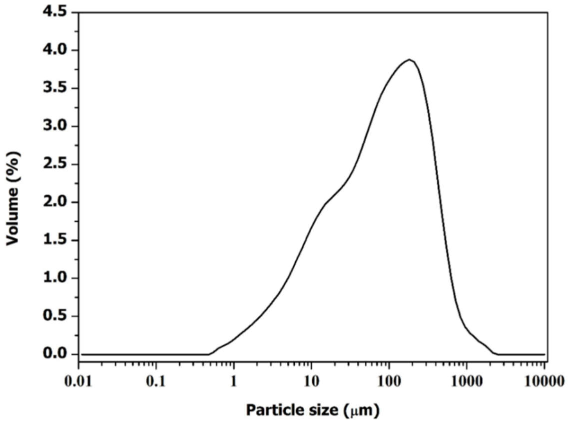

Fig. 3 Size distribution by volume of the synthesized composite

by Hongchao et al. (2011), who synthesized visible light photocatalysts using $ZnSO_4$ impregnated on activated carbon. The potential of ZnO/ZnS nanocomposite as an antioxidant and anti-hemolytic has been reported in the literature (Khan et al., 2025).

The optical properties of the composite were studied by determining the band gap (Eg) using the Kubelka-Munk equation (1) and the Tauc relation (2), which was plotted $(\alpha h\nu)^2$ against $h\nu$ (energy) (Fig. 6).

$$F\left(R_{\infty}\right) = \frac{\left(1 - R_{\infty}\right)^2}{2R_{\infty}} \tag{1}$$

$$\left[F\left(R_{\infty}\right)h\nu\right]^2 = A\ (h\nu - Eg) \tag{2}$$

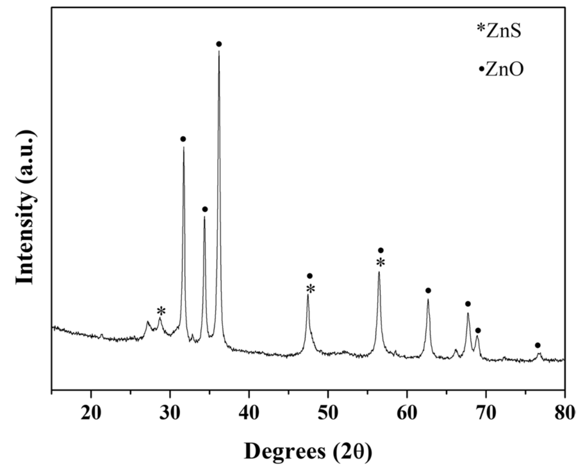

Fig. 5 X-ray diffraction pattern of the synthesized composite

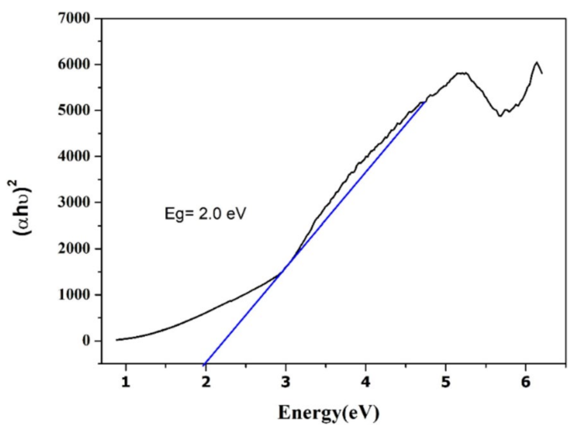

Fig. 6 Tauc plot for or the composite under studied

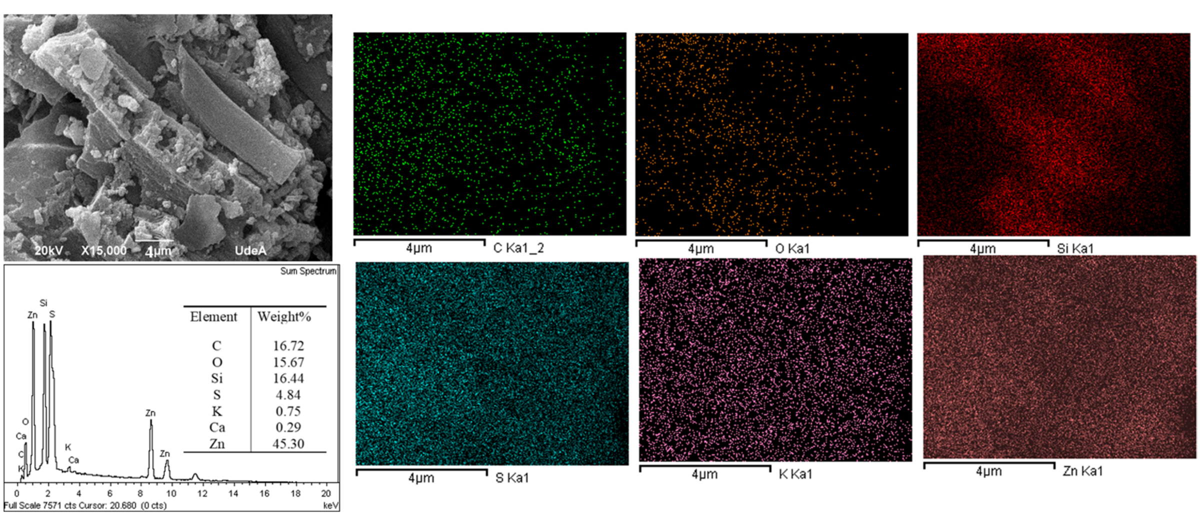

Fig. 4 SEM and elemental mapping with EDX results for the synthesized composite

$F(R_{\infty})$ is the Kubelka-Munk function; R_{∞} the reflectance, and A is an empirical constant.

The tangent curve was extrapolated to the x-axis, obtaining an Eg value of 2.0 eV. Chankhanittha et al. (2023) reported that heterojunctions of ZnS/ZnO with bandgaps between 3.09 and 3.11 eV, presented satisfactory photocatalytic performance for environmental remediation. In another study (Thirumoolan et al., 2024), a chemical precipitation method was used to obtain Ni-dopped ZnO supported on activated carbon with a bandgap of 2.76 eV. These results show that carbon can reduce the band gap energy of non-metal compounds.

3.2 Assessment of the Composite Potential Use in the Photocatalytic Removal of Sildenafil

The potential use of the composite in photocatalytic reactions was evaluated by considering its ability to remove SDF from aqueous solutions. For this purpose, the material was activated using simulated sunlight (290 - 800 nm). Initially, screening tests were performed, varying the catalyst dose to evaluate the contribution of adsorption and photolysis mechanisms in removing the contaminant. From Fig. 7, it can be inferred that the joint action (synergistic effect) of the sunlight radiation and the presence of the composite promotes a higher removal of SDF compared to the individual effects of each factor.

3.3 Effect of the Composite Initial Dose on SDF Removal

The initial catalyst dose on SDF removal was evaluated between 0.05 and 0.5 g/L under a solution pH of 7 and an initial pollutant concentration of 1.0 mg/L. Figure 8 depicts the associated results, from which it can be seen that initially increasing the catalyst dose from 0.05 to 0.1 g/L leads to a more significant removal of SDF. It could be associated with a potential increase in the generation of active sites on the solid surface, promoting the possible elimination of the pollutant. However, as the concentration of the material increases, an inhibitory effect occurs, and the pollutant removal significantly decreases. This may be because a greater amount of composite in suspension could limit the penetration of light into the solution due to a higher opacity and turbidity, which has been reported by several authors regarding the use of materials such as TiO_2 or ZnO in photocatalytic systems (Chakravorty & Roy, 2024; Wang et al., 2022).

3.4 Effect of the Solution pH on SDF Removal

The solution pH is crucial when establishing reaction mechanisms in photocatalytic systems, as it can modify the interactions between the catalyst surface and the contaminant (Chakravorty & Roy, 2024). In this sense, the removal of SDF was studied under three pH conditions (3, 7, and 9), and the results are shown

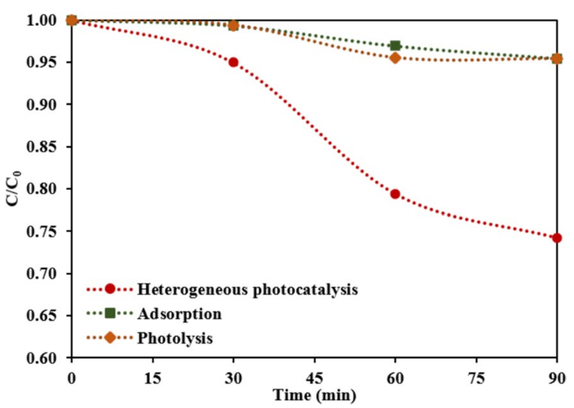

Fig. 7 SDF removal under photocatalysis, adsorption, and photolysis. Pollutant initial concentration 1.0 mg/L, solution pH 7, catalyst dose 0.3 g/L, irradiance 500 W/m^2, 25 °C

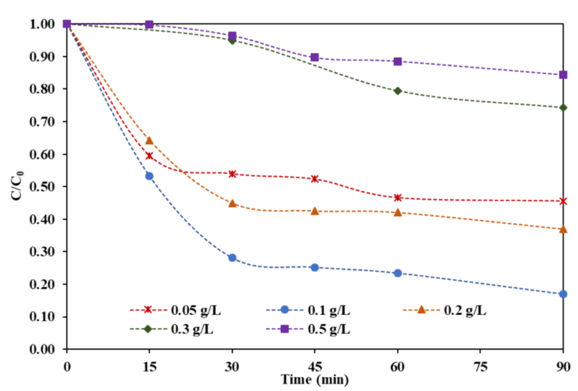

Fig. 8 Effect of composite dose on SDF removal using heterogeneous photocatalysis. Pollutant initial concentration 1 mg/L, solution pH 7, irradiance 500 W/m^2, 25 °C

in Fig. 9. First, it is noted that the removal is significantly lower under acidic conditions, whereas at pH 7 and 9, similar results are achieved after 90 minutes of reaction. It is also observed that the neutrality of the solution is the condition that most favors the pollutant removal. To interpret the results, it is essential to clarify the behavior of the SDF molecule under various pH conditions. Depending on the pH of the medium, the SDF molecule can adopt a positive or a negative charge (Wang et al., 2013). At pH > 9.12, SDF has a negative charge, while at pH < 6.78, it is positive (Abdelalim et al., 2020; Wang et al., 2013). The charge is neutral in the range 6.78 to 9.12, as indicated in Figure 10. On the other hand, the point of zero charge (PZC) of the composite was determined following the method described by Yağmur and Kaya (2021), from which it was established that the PZC for the material is 7.2 (see inset graph in Fig. 9). In this sense, at pH 3, both the SDF molecule and the catalyst surface are positively charged, which would give rise to an electrostatic repulsion; at pH 7, the molecule and the surface of the solid would have zero charge; and at pH 9 both charges would be negative implying that electrostatically the contaminant would be closer to the catalyst surface at pHs close to neutral. Additionally, it has been reported that under alkaline conditions, it is possible to generate a more significant number of radical species (especially the hydroxyl radical, HO●) with the capacity to rapidly oxidize organic compounds (Chakravorty & Roy, 2024), which seems to favor the removal of SDF at pH 9 regardless of the electrostatic repulsion.

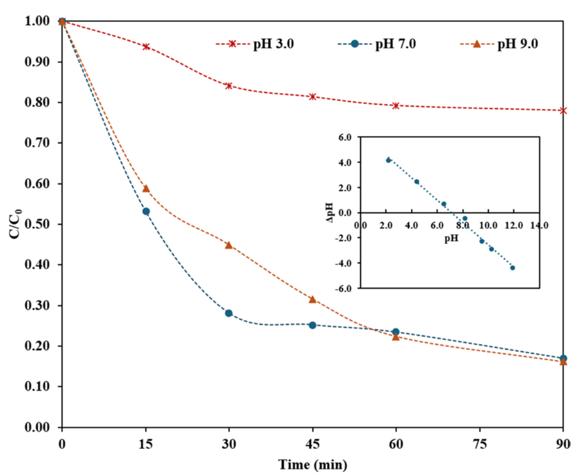

Fig. 9 Effect of the solution pH on SDF removal using heterogeneous photocatalysis. Pollutant initial concentration 1.0 mg/L, catalyst dose 0.1 g/L, irradiance 500 W/m^2, 25 °C. Inset graph: Composite PZC determination

3.5 Assessment of the SDF Removal Mechanism

In general, the performance of heterogeneous photocatalysis in removing organic pollutants from water is associated with three types of mechanisms: (i) the adsorption of contaminants on the catalyst surface, (ii) the breaking of the molecule bonds due to the action of the irradiated light, and (iii) the generation of radicals capable of oxidizing the organic matter present in the solution. In this sense, Fig. 7 allows to infer that mechanisms (i) and (ii) do not significantly affect the removal of SDF under the evaluated conditions, and that it is necessary to establish the role of the possible photo-generated species on the pollutant elimination. During the photocatalytic activation of a material, an excited electron (e^-) moves from the valence band to the conduction band, leaving a hole (h^+) in which the water adsorbed on the surface can give rise to different species such as the HO● radicals, which can react rapidly with different organic compounds and even promote their mineralization (Bodzek et al., 2023; Chakravorty & Roy, 2024). Two control tests, including the presence of isopropanol (iPrOH), were performed to clarify the role of the HO● radicals on SDF removal. iPrOH is known as a

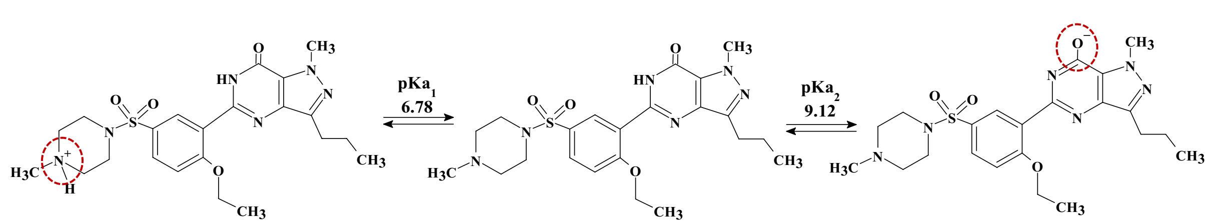

Fig. 10 SDF behavior as function on pH solution

scavenger agent capable of reacting with HO• (Ma et al., 2021). Likewise, some tests were performed using an organic solvent (acetonitrile) instead of water, for identifying the photo-generated holes'role (Tao et al., 2020).

Figure 11 indicates that the presence of iPrOH or carrying out experiments using an organic solvent decreases the extent of pollutant removal. On the one hand, iPrOH would reduce the number of radicals available to oxidize SDF, while the absence of water implies a lower generation of them. Given the above, HO• radicals seem to be the main responsible species for SDF removal under the conditions evaluated in this work.

According to the discussed results, equations 3–10 represent the proposed mechanism of SDF removal under the ZnO-ZnS composite activation using simulated sunlight.

$$ZnO - ZnS + h\nu \rightarrow e^- + h^+ \tag{3}$$

$$e^- + h^+ \rightarrow \text{recombination} \tag{4}$$

$$h^+ + H_2O \rightarrow HO^\bullet + H^+ \tag{5}$$

$$h^+ + OH^- \rightarrow HO^\bullet \tag{6}$$

$$h^+ + SDF \rightarrow \text{Degradation byproducts} \tag{7}$$

$$HO^\bullet + SDF \rightarrow \text{Degradation byproducts} \tag{8}$$

$$e^- + O_2 \rightarrow O_2^- \bullet \tag{9}$$

$$SDF + HO^\bullet + O_2^- \bullet \rightarrow \text{Degradation byproducts} + CO_2 + H_2O \tag{10}$$

3.6 Evaluation of Catalyst Reuse

An important aspect when evaluating the performance of a new material in removing organic contaminants is to consider its reuse during various cycles, which could represent advantages from an economic and environmental point of view since it would not be necessary to dispose the material after each use (Cseri, 2024; Kamari & Ghiaci, 2016). Thus, the reuse of the composite in the removal of SDF was evaluated during five different cycles. The fresh material (cycle 1) was used for 90 min; then, it was centrifuged, filtered, washed with water and ethanol, and finally dried in an air atmosphere. Subsequently, it was used in a second cycle for removing SDF, and after 90 min, it was recovered and used until five cycles were completed. Figure 12 shows that in all cycles, the SDF removal was higher than 50 %, indicating that the material is promising even in terms of its reuse. One reason for these results could be related to the fact that the removal of the

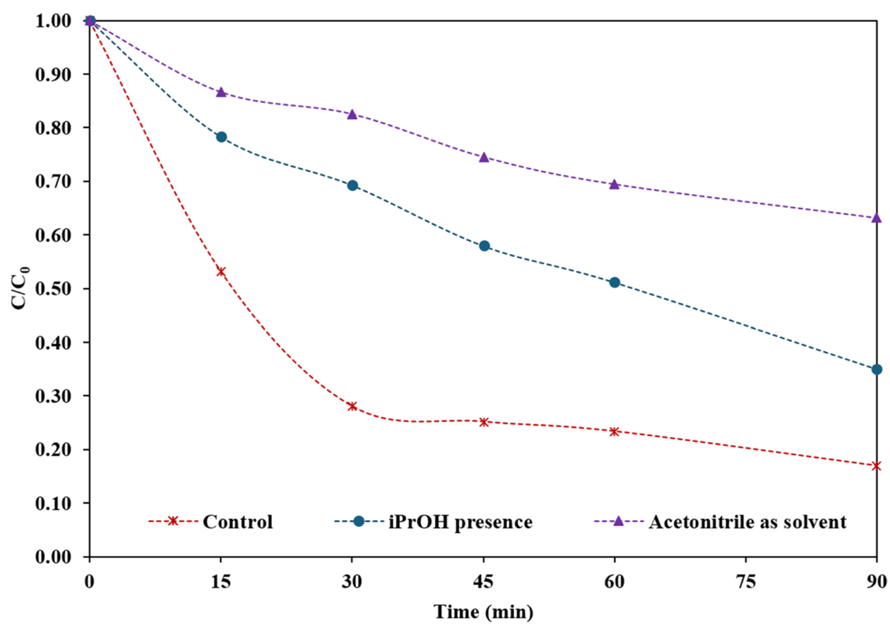

Fig. 11 Evaluation of the mechanism of SDF removal using heterogeneous photocatalysis. Pollutant initial concentration 1.0 mg/L, catalyst dose 0.1 g/L, solution pH 7, iPrOH 100 mg/L, irradiance 500 W/m^2, 25 °C

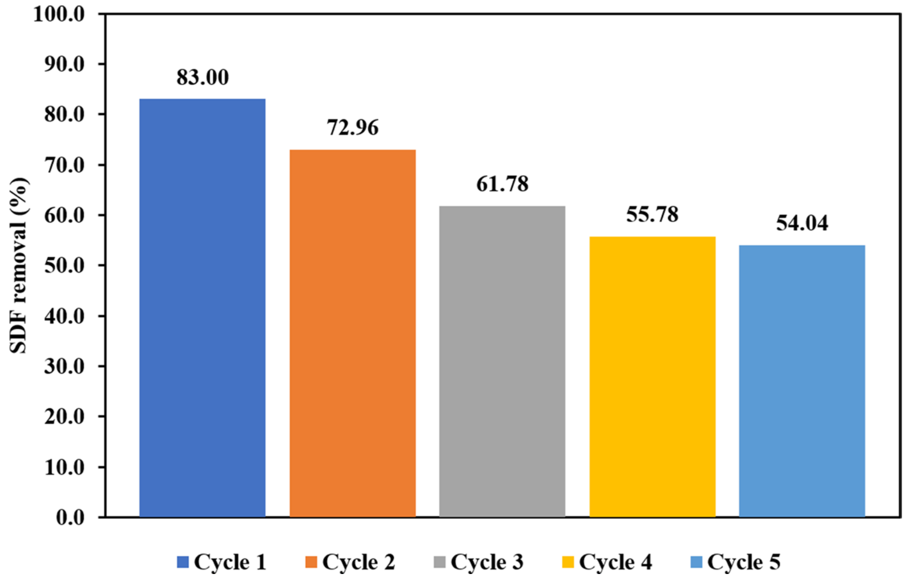

Fig. 12 Evaluation of the composite reuse on the SDF removal using heterogeneous photocatalysis. Pollutant initial concentration 1.0 mg/L, catalyst dose 0.1 g/L, solution pH 7, irradiance 500 W/m^2, 25 °C

contaminant is presumed to be a result of its oxidation after the generation of HO• radicals and not by its absorption on the catalyst surface, which implies that the physisorbed water reacts with the photogenerated holes producing radicals, which once released leave free spaces in the material, favoring the continued generation of h$^+$ - e$^-$ pairs after photoactivation.

3.7 Antibacterial Activity of the Synthesized Composite

The antibacterial performance of the composite against *E. Coli* and *S. Aureus* was evaluated using the agar disk diffusion method. Figures 13 and 14 show the results with several composite dose in contact with *E. coli* and *S. aureus*.

In both figures, an inhibitory zone is observed around the composite samples. This behavior implies that the solid has antibacterial activity (Yagoub et al., 2022). Table 1 presents the results of quantifying the inhibition zones and their comparison with the positive control (tetracycline). The inhibition diameters are between 14.5 and 18.5 mm for *E. Coli* and 14.5 and 20.5 mm for *S. aureus*, indicating no appreciable differences in the inhibitory behavior of the composite against gram-negative or gram-positive bacteria. However, a trend of increasing antibacterial action is observed as the quantity of composite increases.

Some authors (Fu et al., 2014; Kumar et al., 2023; Pasquet et al., 2014) have reported various mechanisms of action to explain the antibacterial properties

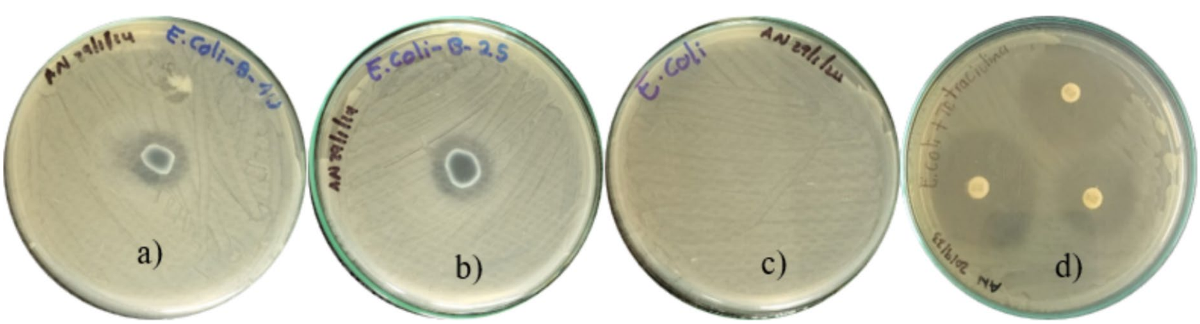

Fig. 13 Disc diffusion tests for the evaluation of the material antibacterial activity against *E. coli*. Composite dose: **a** 10 mg, **b** 25 mg, **c** controls *E. coli*, and **d** tetracycline (30 µg). Inoculation time 24 h

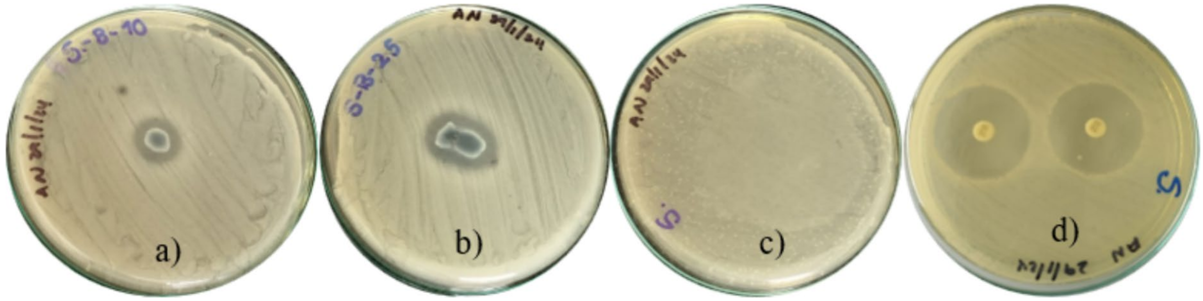

Fig. 14 Disc diffusion tests for the evaluation of the material antibacterial activity against *S. aureus*. Composite dose: **a** 10 mg, **b** 25 mg; **c** controls *S. aureus*, **d** tetracycline (30 μg). Inoculation time 24 h

Table 1 Inhibition diameter values in mm for the composite and the positive control (tetracycline) on *E. Coli* and *S. aureus*

Bacterial strain	Tetracycline (30.0 μg)	Composite (10.0 mg)	Composite (25.0 mg)
E. coli	30 ± 0.0	14.5 ± 0.7	18.5 ± 0.7
S. aureus	30 ± 0.6	14.5 ± 0.7	20.5 ± 0.7

Value measured by triplicate

of ZnO composites. It is supposed that the generation of reactive oxygen species such as H_2O_2, OH^-, and O^{2-} causes DNA and protein damage, lipid peroxidation, and unregulated cell signaling. The release of Zn^{2+} ions through direct interaction with bacterial membranes enhances permeability; additionally, Zn^{2+} ions can interact with nucleic acids and deactivate enzymes involved in the bacterial respiration system.

4 Conclusions

This work investigates the antibacterial and photocatalytic properties of a novel composite synthesized through thermal treatment at 500 °C from banana peels and zinc sulfate. The high thermal material with micro-mesoporosity contained carbon, ZnO, and ZnS species. Evaluation of the potential use of the catalyst in removing sildenafil from aqueous solutions indicates that it could promote the generation of hydroxyl radicals, which subsequently oxidize the pollutant. Some of the identified advantages of the material include the possibility of being activated using sunlight radiation and its ability to remove more than 50 % of sildenafil, even after five cycles of use. The composite also showed potential antibacterial activity, which has significant implications for the development of sustainable and cost-effective antimicrobial agents. This research could contribute to combating antibiotic resistance while repurposing agricultural waste, promoting environmental sustainability, and public health.

CrediT Authorships Contributions Assessment MM: conceptualization, investigation, methodology, and writing – original draft; LFV: investigation and methodology; CQ: investigation and methodology; HZ: methodology, writing – review & editing; ALV: resources, funding acquisition, writing – review & editing; and GAP: writing – review & editing, resources, funding acquisition.

Acknowledgments The authors want to acknowledge financial support from Universidad de Antioquia (UdeA) and to El Carmen de Viboral UdeA campus for allowing the use of their facilities to conduct antibacterial activity testing.

Funding Open Access funding provided by Colombia Consortium.

Data Availability Data will be made available on request.

Declarations

Competing Interest The authors declare that they have no known competing financial interests or personal relationships that could have appeared to influence the information reported in this paper.

References

Abdelalim, L. R., Elnaggar, Y. S. R., & Abdallah, O. Y. (2020). Oleosomes Encapsulating Sildenafil Citrate as Potential Topical Nanotherapy for Palmar Plantar Erythrodysesthesia with High Ex vivo Permeation and Deposition. *AAPS PharmSciTech, 21*(8), 310. https://doi.org/10.1208/s12249-020-01862-2

Abdullah, H., Ginting, R. T., Shuwanto, H., & Kuo, D. H. (2022). Banana peel biowaste-derived carbon composited with Zn (O, S) for solar-light photocatalytic hydrogen generation. *International Journal of Hydrogen Energy, 47*(97), 41021–41033. https://doi.org/10.1016/j.ijhydene.2022.09.184

Ali, S., Saleem, S., Salman, M., & Khan, M. (2020). Synthesis, structural and optical properties of ZnS–ZnO nanocomposites. *Materials Chemistry and Physics, 248*, 122900. https://doi.org/10.1016/j.matchemphys.2020.122900

Alphanoda, A. F., Pane, E. A., & Riyanto, A. (2024). The Role of Banana Peel Surface Pores through Increasing Temperature for Efficient Hydrogen Production. *Journal of Mechanical Engineering Science and Technology*, (8), 421–433.

Anyama, C. A., Ita, B. I., Ayi, A. A., Louis, H., Okon, E. E. D., Ogar, J. O., & Oseghale, C. O. (2021). Experimental and Density Functional Theory Studies on a Zinc(II) Coordination Polymer Constructed with 1,3,5-Benzenetricarboxylic Acid and the Derived Nanocomposites from Activated Carbon. *ACS Omega, 6*(43), 28967–28982. https://doi.org/10.1021/acsomega.1c04037

Atilgan, A., Krakowiak-Bal, A., Ertop, H., Saltuk, B., & Malinowski, M. (2023). The Energy Potential of Waste from Banana Production: A Case Study of the Mediterranean Region. *Energies, 16*(14), 5244. https://doi.org/10.3390/en16145244

Barna, T., Szucs, K. F., Mirdamadi, M., & Gaspar, R. (2023). The combined uterorelaxant effect of sildenafil and terbutalin in the rat: The potential benefit of co-administration of low doses. *Heliyon, 9*(12), e22488. https://doi.org/10.1016/j.heliyon.2023.e22488

Bianchini Fulindi, R., Domingues Rodrigues, J., Lemos Barbosa, T. W., Goncalves Garcia, A. D., de Almeida La Porta, F., Pratavieira, S., Chiavacci, L. A., Pessoa Araújo Junior, J., da Costa, P. I., & Martinez, L. R. (2023). Zinc-Based Nanoparticles Reduce Bacterial Biofilm Formation. *Microbiology Spectrum, 11*(2). https://doi.org/10.1128/spectrum.04831-22

Bisauriya, R., Verma, D., & Goswami, Y. C. (2018). Optically important ZnS semiconductor nanoparticles synthesized using organic waste banana peel extract and their characterization. *Journal of Materials Science: Materials in Electronics, 29*(3), 1868–1876. https://doi.org/10.1007/s10854-017-8097-6

Bodzek, M., Konieczny, K., & Kwiecińska-Mydlak, A. (2023). Recent advances in water and wastewater disinfection by nano-photocatalysis. *Desalination and Water Treatment, 305*, 2–16. https://doi.org/10.5004/dwt.2023.29390

Chakravorty, A., & Roy, S. (2024). A review of photocatalysis, basic principles, processes, and materials. *Sustainable Chemistry for the Environment, 8*, 100155. https://doi.org/10.1016/j.scenv.2024.100155

Chankhanittha, T., Watcharakitti, J., Piyavarakorn, V., Johnson, B., Bushby, R. J., Chuaicham, C., Sasaki, K., Nijpanich, S., Nakajima, H., Chanlek, N., & Nanan, S. (2023). ZnO/ZnS photocatalyst from thermal treatment of ZnS: Influence of calcination temperature on development of heterojunction structure and photocatalytic performance. *Journal of Physics and Chemistry of Solids, 179*, 111393. https://doi.org/10.1016/j.jpcs.2023.111393

Cseri, L. (2024). Recovery and Reuse of Metal Complex Catalysts. In *Reference Module in Chemistry, Molecular Sciences and Chemical Engineering*. Elsevier. https://doi.org/10.1016/B978-0-443-15742-4.00045-4

Das, A. K., Mitra, K., Conte, A. J., Sarker, A., Chowdhury, A., & Ragauskas, A. J. (2024). Lignin - A green material for antibacterial application — A review. *International Journal of Biological Macromolecules, 261*, 129753. https://doi.org/10.1016/j.ijbiomac.2024.129753

Eswaran, P., Madasamy, P. D., Pillay, K., & Brink, H. (2024). Sunlight-driven photocatalytic degradation of methylene blue using ZnO/biochar nanocomposite derived from banana peels. *Biomass Conversion and Biorefinery*, 1–21. https://doi.org/10.1007/s13399-024-05999-z

Farias, K. C. S., Guimarães, R. C. A., Oliveira, K. R. W., Nazário, C. E. D., Ferencz, J. A. P., & Wender, H. (2023). Banana Peel Powder Biosorbent for Removal of Hazardous Organic Pollutants from Wastewater. *Toxics, 11*(8), 664. https://doi.org/10.3390/toxics11080664

Fu, P. P., Xia, Q., Hwang, H.-M., Ray, P. C., & Yu, H. (2014). Mechanisms of nanotoxicity: Generation of reactive oxygen species. *Journal of Food and Drug Analysis, 22*(1), 64–75. https://doi.org/10.1016/j.jfda.2014.01.005

Garay-Rodríguez, L. F., Luévano-Hipólito, E., & Torres-Martínez, L. M. (2023). Renewable formic acid production from CO2 reduction using green ZnO nanoarchitectures. *Materials Science in Semiconductor Processing, 161*, 107458. https://doi.org/10.1016/j.mssp.2023.107458

Gomez, G. E., Hamer, M., Regiart, M. D., Tortella, G. R., Seabra, A. B., Soler Illia, G. J. A. A., & Fernández-Baldo, M. A. (2024). Advances in Nanomaterials and Composites Based on Mesoporous Materials as Antimicrobial Agents: Relevant Applications in Human Health. *Antibiotics, 13*(2), 173. https://doi.org/10.3390/antibiotics13020173

Hongchao, M., Jihui, H., Yinghuan, F., Yu, S., Chunling, Y., & Xiaoli, D. (2011). Synthesis of visible light responsive ZnO–ZnS/C photocatalyst by simple carbothermal reduction. *Applied Catalysis B: Environmental, 102*(3-4), 417–423. https://doi.org/10.1016/j.apcatb.2010.12.014

Huët, M. A. L., Phul, I. C., Goonoo, N., Li, Z., Li, X., & Bhaw-Luximon, A. (2024). Lignin–cellulose complexes derived from agricultural wastes for combined antibacterial and tissue engineering scaffolds for cutaneous leishmaniasis wounds. *Journal of Materials Chemistry B, 12*(22), 5496–5512. https://doi.org/10.1039/D4TB00458B

Kamari, Y., & Ghiaci, M. (2016). Incorporation of TiO2 coating on a palladium heterogeneous nanocatalyst. A new method to improve reusability of a catalyst. *Catalysis Communications, 84*, 16–20. https://doi.org/10.1016/j.catcom.2016.05.018

Khan, T. F., Muhyuddin, M., Irum, S., Ali, M. A., Husain, S. W., & Basit, M. A. (2025). Comparing the antioxidant and hemolytic activity of wet-chemically synthesized ZnO, ZnS, and ZnO/ZnS nanocomposite. *Inorganic Chemistry Communications, 174*, 113902. https://doi.org/10.1016/j.inoche.2025.113902

Korni, R. D., Boddepalli, T., Elusuri, J., & Panda, J. (2023). Banana Peel: A potential waste product with numerous pharmacological activities. *GSC Biological and Pharmaceutical Sciences, 23*(2), 160–174. https://doi.org/10.30574/gscbps.2023.23.2.0190

Kumar, M., Sridharan, S., Sawarkar, A. D., Shakeel, A., Anerao, P., Mannina, G., Sharma, P., & Pandey, A. (2023). Current research trends on emerging contaminants pharmaceutical and personal care products (PPCPs): A comprehensive review. *Science of the Total Environment, 859*, 160031. https://doi.org/10.1016/J.SCITOTENV.2022.160031

Li, K., Zhong, W., Li, P., Ren, J., Jiang, K., & Wu, W. (2023). Antibacterial mechanism of lignin and lignin-based antimicrobial materials in different fields. *International Journal of Biological Macromolecules, 252*, 126281. https://doi.org/10.1016/j.ijbiomac.2023.126281

Lobo, F. C. M., Franco, A. R., Fernandes, E. M., & Reis, R. L. (2021). An Overview of the Antimicrobial Properties of Lignocellulosic Materials. *Molecules, 26*(6), 1749. https://doi.org/10.3390/molecules26061749

Luo, J., Huang, K., Zhou, X., & Xu, Y. (2020). Preparation of highly flexible and sustainable lignin-rich nanocellulose film containing xylonic acid (XA), and its application as an antibacterial agent. *International Journal of Biological Macromolecules, 163*, 1565–1571. https://doi.org/10.1016/j.ijbiomac.2020.07.281

Ma, D., Yi, H., Lai, C., Liu, X., Huo, X., An, Z., Li, L., Fu, Y., Li, B., Zhang, M., Qin, L., Liu, S., & Yang, L. (2021). Critical review of advanced oxidation processes in organic wastewater treatment. *Chemosphere, 275*, 130104. https://doi.org/10.1016/J.CHEMOSPHERE.2021.130104

Melanie, K., Nazlia, S., Saputra, J., Purnama Febri, S., & Rezvani Aprita, I. (2024). The effect of banana peel flour (Musa paradisiaca) as additional feed raw materials for common carp (Cyprinus carpio). *BIO Web of Conferences, 87*, 03024. https://doi.org/10.1051/bioconf/20248703024

Midolo, P. D., Turnidge, J., Lambert, J. R., & Bell, J. M. (1995). Validation of a modified Kirby-Bauer disk diffusion method for metronidazole susceptibility testing of Helicobacter pylori. *Diagnostic Microbiology and Infectious Disease, 21*(3), 135–140. https://doi.org/10.1016/0732-8893(95)00066-J

Mishra, V., Kesharwani, S., Chivate, M., Chauhan, A. K., & Mishra, V. (2023). Development of Novel Biofertilizer by Combining the Banana Waste and Cyanobacteria in Sustainable Agriculture. *International Journal of Food and Fermentation Technology, 13*(1), 69–86. https://doi.org/10.30954/2277-9396.01.2023.7

Nesterov, D., Barrera-Martínez, I., Martínez-Sánchez, C., Sandoval-González, A., & Bustos, E. (2024). Approaching the circular economy: Biological, physicochemical, and electrochemical methods to valorize agro-industrial residues, wastewater, and industrial wastes. *Journal of Environmental Chemical Engineering, 12*(5), 113335. https://doi.org/10.1016/j.jece.2024.113335

Pasquet, J., Chevalier, Y., Pelletier, J., Couval, E., Bouvier, D., & Bolzinger, M.-A. (2014). The contribution of zinc ions to the antimicrobial activity of zinc oxide. *Colloids and Surfaces A: Physicochemical and Engineering Aspects, 457*, 263–274. https://doi.org/10.1016/j.colsurfa.2014.05.057

Pullapukuri, K., & Kumar, S. (2023). Green synthesis of zinc oxide nanoparticles with biological activity and their charactyerization by using banana peel extract. *Chelonian Research Foundation, 18*(2), 689–701 https://www.acgpublishing.com/index.php/CCB/article/view/56

Serna-Jiménez, J. A., Siles López, J. Á., de los Ángeles Martín Santos, M., & Chica Pérez, A. F. (2023). Exploiting waste derived from Musa spp. processing: Banana and plantain. *Biofuels, Bioproducts and Biorefining, 17*(4), 1046–1067. https://doi.org/10.1002/bbb.2475

Singh, R., Chandra, R., Bose, M., & Luthra, P. M. (2002). Antibacterial activity of Curcuma longa rhizome extract on pathogenic bacteria. *Current Science, 83*(6), 737–740 http://www.jstor.org/stable/24106150

Tao, C., Jia, Q., Han, B., & Ma, Z. (2020). Tunable selectivity of radical generation over TiO2 for photocatalysis. *Chemical Engineering Science*. https://doi.org/10.1016/j.ces.2019.115438

Thirumoolan, D., Ragupathy, S., Renukadevi, S., Rajkumar, P., Rai, R. S., Saravana Kumar, R. M., Hasan, I., Durai, M., & Ahn, Y.-H. (2024). Influence of nickel doping and cotton stalk activated carbon loading on structural, optical, and photocatalytic properties of zinc oxide nanoparticles. *Journal of Photochemistry and Photobiology A: Chemistry, 448*, 115300. https://doi.org/10.1016/j.jphotochem.2023.115300

T-Thienprasert, N. P., T-Thienprasert, J., Ruangtong, J., Jaithon, T., Srifah Huehne, P., & Piasai, O. (2021). Large Scale Synthesis of Green Synthesized Zinc Oxide Nanoparticles from Banana Peel Extracts and Their Inhibitory Effects against Colletotrichum sp., Isolate KUFC 021, Causal Agent of Anthracnose on Dendrobium Orchid. *Journal of Nanomaterials, 2021*, 1–10. https://doi.org/10.1155/2021/5625199

United Nations (UN) Environment programm. (2024). World must move beyond waste era and turn rubbish into resource: UN Report.

Villa, A. L., & Mediavilla, M. (2023). Evaluation of the Isomerization of α-Pinene Epoxide to Campholenic Aldehyde Using a Catalyst Obtained from Orange Peels (Citrus sinensis). *Revista Tecnica De La Facultad De Ingenieria Universidad Del Zulia*, e234603. https://doi.org/10.22209/rt.v46a03

Wang, C. C., Gómez, R. A., & Fernandez, L. P. (2013). Determination of sildenafil by preconcentration on surfactant coated polymeric resin followed by spectrofluorimetry. *Journal of Pharmaceutical Analysis, 3*(3), 173–179. https://doi.org/10.1016/j.jpha.2012.11.001

Wang, H., Li, X., Zhao, X., Li, C., Song, X., Zhang, P., Huo, P., & Li, X. (2022). A review on heterogeneous photocatalysis for environmental remediation: From semiconductors to modification strategies. *Chinese Journal of Catalysis, 43*(2), 178–214. https://doi.org/10.1016/S1872-2067(21)63910-4

World Health Organization (WHO). (2023). WHO urges investing in "One Health" actions for better health of the people and the planet.

Yağmur, H. K., & Kaya, İ. (2021). Synthesis and characterization of magnetic ZnCl2-activated carbon produced from coconut shell for the adsorption of methylene blue. *Journal of Molecular Structure, 1232*, 130071. https://doi.org/10.1016/j.molstruc.2021.130071

Yagoub, A. E. A., Al-Shammari, G. M., Al-Harbi, L. N., Subash-Babu, P., Elsayim, R., Mohammed, M. A., Yahya, M. A., & Fattiny, S. Z. A. (2022). Antimicrobial Properties of Zinc Oxide Nanoparticles Synthesized from Lavandula pubescens Shoot Methanol Extract. *Applied Sciences, 12*(22), 11613. https://doi.org/10.3390/app122211613

Zeghoud, S., Hemmami, H., Ben Seghir, B., Ben Amor, I., Kouadri, I., Rebiai, A., Messaoudi, M., Ahmed, S., Pohl, P., & Simal-Gandara, J. (2022). A review on biogenic green synthesis of ZnO nanoparticles by plant biomass and their applications. *Materials Today Communications, 33*, 104747. https://doi.org/10.1016/j.mtcomm.2022.104747

Zeng, Q., Jia, Z., Liu, X., & Cheng, J. (2023). A novel 1T-2H MoS2/NaBi(MoO4)2 alternating-phase piezoelectric composites for high-efficient ultrasound-drived piezoelectric catalytic removal of Sildenafil. *Process Safety and Environmental Protection, 179*, 314–328. https://doi.org/10.1016/j.psep.2023.09.021

Zhang, W., Tu, G., Zhang, H., Zheng, Y., & Yang, L. (2014). Synthesis and antibacterial activity of mesoporous zinc oxide particle with high specific surface area. *Materials Letters, 114*, 119–121. https://doi.org/10.1016/j.matlet.2013.09.028

Zizzamia, A. R., Tesoro, C., Bianco, G., Bufo, S. A., Ciriello, R., Brienza, M., Scrano, L., & Lelario, F. (2024). Efficient photooxidation processes for the removal of sildenafil from aqueous environments: A comparative study. *Case Studies in Chemical and Environmental Engineering, 9*, 100708. https://doi.org/10.1016/j.cscee.2024.100708